Seismic Design and Testing of Propped Rocking Wall Systems

A. Nicknam
Ph.D. Candidate, Dept. of Civil, Structural and Environmental Eng., University at Buffalo, Buffalo, New York, USA, Email: anicknam@buffalo.edu

A. Filiatrault
Professor, Dept. of Civil, Structural and Environmental Eng., University at Buffalo, Buffalo, New York, USA, Email: af36@buffalo.edu

SUMMARY:
A direct displacement-based design (DDBD) methodology is described for Propped Rocking Wall (PRW) systems. A PRW represents a novel seismic force-resisting system that combines passive supplemental damping devices with unbonded post-tensioned concrete rocking walls. The key aspect of the proposed design procedure is the closed-form derivation of the stabilized hysteretic response of PRWs under reverse cyclic loading. This allows the direct application of the DDBD procedure to satisfy desired displacement performance objectives under prescribed levels of seismic intensity. The efficiency of the proposed design procedure and the performance of PRWs are evaluated experimentally through an ongoing earthquake simulator experimental program on a 1:3 scaled PRW specimen designed using the proposed DDBD procedure. Results from the preliminary nonlinear dynamic analyses on the test structure are presented in order to demonstrate its performance under strong ground shaking.

Keywords: Concrete rocking wall, displacement-based design, passive supplemental damping

1. DESCRIPTION OF PROPPED ROCKING WALLS

Propped Rocking Walls (PRWs) is an innovative seismic force-resisting system proposed by Fathali (2009) that combines passive supplemental damping with unbonded post-tensioned rocking concrete walls. The system, as illustrated in Fig. 1.1, consists of a self-standing slender concrete wall, post-tensioned by unbonded steel (PT) bars and propped near its top by multi-story diagonal steel braces. These braces are latterly supported by the floor slabs of the building to reduce their overall slenderness ratio. As indicated in Fig. 1.1, each group of braces on each side of the system (referred herein as "steel props") can incorporate several hysteretic dampers in series. During ground shaking, the hysteretic dampers within the steel props are activated to dissipate energy. The rocking of the wall at its base-foundation interface avoids the formation of a plastic hinge in the wall panel.

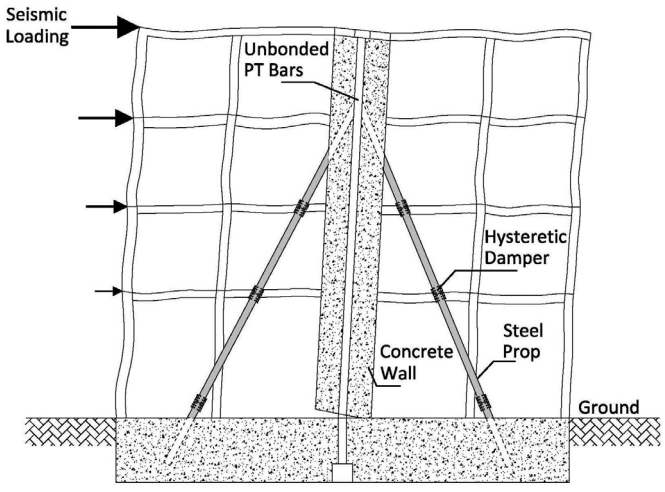

Figure 1.1. General layout and deformed shape of a propped rocking wall.

PRWs represent an extension of the existing Propped Shear Wall (PSWs) system, which has been used in the seismic retrofit of several buildings in the San Francisco Bay Area, CA, U.S.A. (Wolfe *et al*., 2001). In PSWs, conventional concrete shear walls are used and are allowed to hinge at their base for rare and intense ground shaking. The main objectives of this paper are to develop a direct displacement-based design (DDBD) methodology for PRWs and evaluate numerically and experimentally their seismic performance under strong ground shaking.

2. CLOSED-FORM HYSTERETIC RESPONSE OF PROPPED ROCKING WALLS

The behavior of PRWs under cyclic loading depends mostly on the behavior of two of its main components: 1) the PT bars and 2) the hysteretic dampers. Figs. 2.1 (a) and (b) show the free-body diagram of a PRW at maximum response and the base shear-roof displacement hysteretic response of the system under reverse cyclic loading, respectively.

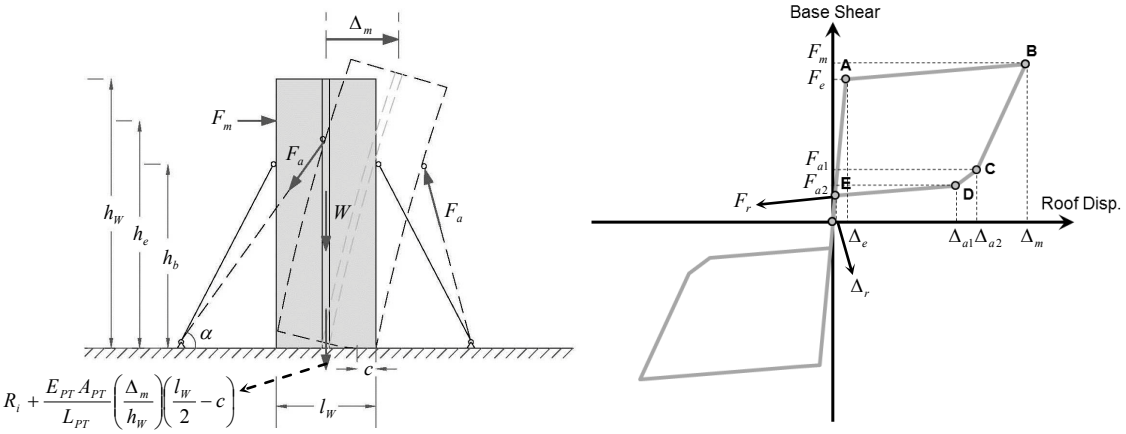

Figure 2.1. (a) The free-body diagram of a PRW at maximum response; and (b) The schematic layout of the stabilized hysteretic response of a PRW system.

A closed-form solution based on small-displacements theory is derived for the stabilized hysteretic response of PRWs shown in Fig. 2.1 (b). As shown in the figure, the hysteretic response of PRWs is governed by five distinct force-displacement coordinates (points A, B, C, D and E). Closed-formed solutions for each of these coordinates based on the force-displacement coordinates at maximum response ($F_m - \Delta_m$) are summarized in Table 2.1.

Table 2.1. Summary of the closed-form solution for different states of the hysteretic response of PRWs.

Point	Roof Displacement	Base Shear
A	$\Delta_e = \frac{1}{2}\left[\frac{h_W^3}{3E_cI_gh_e}\left(\frac{(W+R_i)(l_W-c)}{2}+F_a(2h_b\cos\alpha+l_W\sin\alpha)\right)\times\frac{h_W}{h_e}\right]$	$F_e = F_m - \left(\frac{E_{PT}A_{PT}l_W^2}{4h_Wh_eL_{PT}}-\frac{W+R_i}{2h_e}\right)(\Delta_m-\Delta_e)$
B	Δ_m	$F_m = \frac{1}{h_e}\left((W+R_i)\left(\frac{l_W-c}{2}-\frac{\Delta_m}{2}\right)+2F_ah_b\cos\alpha+F_al_W\sin\alpha+\frac{E_{PT}A_{PT}}{L_{PT}}\left(\frac{\Delta_m}{h_W}\right)\left(\frac{l_W}{2}-c\right)\left(\frac{l_W-c}{2}\right)\right)$
C	$\Delta_{a1} = \Delta_m - \frac{F_ah_W}{k_b(l_W\sin\alpha+h_b\cos\alpha)}$	$F_{a1} = F_m - 2\left[\frac{1}{h_Wh_e}\left(k_b(l_W\sin\alpha+h_b\cos\alpha)^2+k_b(h_b\cos\alpha)^2+\left(\frac{E_{PT}A_{PT}}{L_{PT}}\right)\frac{l_W^2}{4}-\frac{(W+R_i)h_W}{2}\right)\right]\Delta'_{a1}$
D	$\Delta_{a2} = \Delta_m - \frac{F_ah_W}{k_bh_b\cos\alpha}$	$F_{a2} = F_m - 2\left[\frac{1}{h_Wh_e}\left(k_b(h_b\cos\alpha)^2+\left(\frac{E_{PT}A_{PT}}{L_{PT}}\right)\frac{l_W^2}{4}-\frac{(W+R_i)h_W}{2}\right)\right](\Delta'_{a2}-\Delta'_{a1})$
E	$\Delta_r = \frac{F_r}{F_e}\Delta_e$	$F_r = \frac{F_{a2}L_{PT}-E_{PT}A_{PT}(\Delta_m-2\Delta_{a2})}{L_{PT}-\frac{E_{PT}A_{PT}\Delta_e}{F_e}}$

Self-centering of a PRW occurs if the residual force, F_r, is positive. This condition can be written in terms of a contribution ratio, λ, as:

$$\lambda = \frac{F_e + F_r}{F_e - F_r} \geq 1 \tag{2.1}$$

In the equations presented in Table 2.1, E_c and I_g are the elastic modulus and gross moment of inertia of the wall, respectively; c is the neutral axis depth at the wall base section; h_e is the effective height of the wall defined as the height of the resultant of the first modal lateral forces measured from the wall base; W is the weight of the wall; R_i is the initial prestressing force in the PT bars; l_W and h_W are respectively the length and height of the wall; F_a is the activation force of the hysteretic dampers (assumed the same for all dampers); α is the horizontal inclination angle of the braces; h_b is the vertical height of the steel props from the wall base; k_b is the axial stiffness of the steel props; and E_{PT}, A_{PT} and L_{PT} are the elastic modulus, cross-sectional area and unbonded length of the PT bars, respectively.

3. DIRECT DISPLACEMENT-BASED DESIGN OF PROPPED ROCKING WALLS

A Direct Displacement-Based Design (DDBD) procedure was developed for PRWs and is described in this section. DDBD was originally proposed by Priestley (1993) and has now been applied to a variety of seismic force-resisting systems. The primary design variables of the DDBD procedure are estimates of the inelastic deformations in the structural elements, which are considered the best indicators of seismic damage. Fig. 3.1 illustrates the four main steps in the DDBD procedure applied to PRWs. These steps are briefly described below.

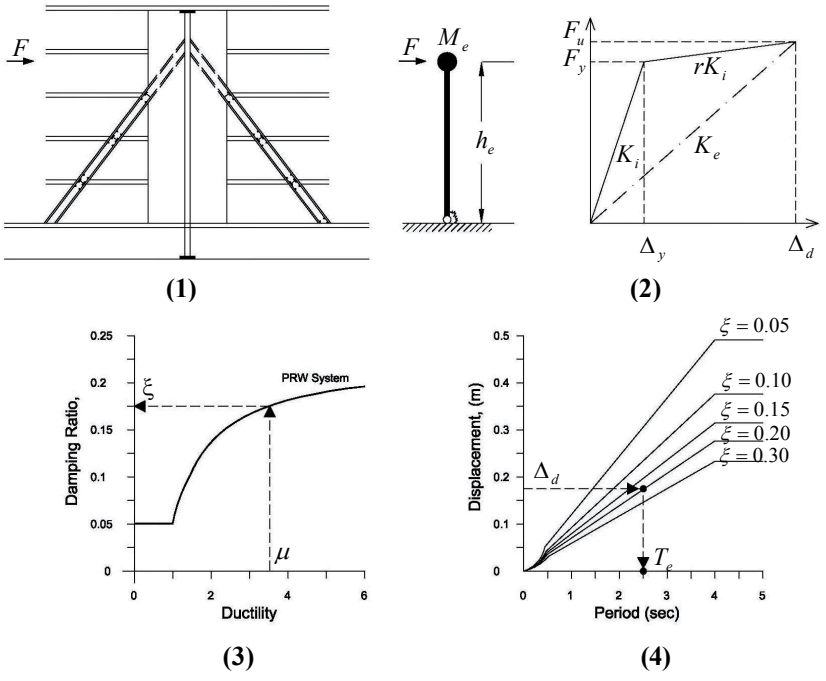

Figure 3.1. Basic steps of Direct Displacement-Based Design (DDBD) of PRWs.

The first step of the DDBD procedure is to develop an equivalent SDOF representation of the PRW under design. This is achieved through the knowledge of the mass distribution and the displacement profile of the PRW at maximum response. The displacement shape (or displacement profile) of the PRW system under design is developed based on a design story drift value set by the designer at the beginning of the design process to insure acceptable levels of deformation for a given level of intensity. In the case of a PRW, the displacement shape at maximum response consists of flexural

deformations of the wall under an inverse triangular lateral force distribution representing the effect of inertia forces, $\Delta_{i\text{-}flexI}$, and under the horizontal components of the activation loads in the hysteretic dampers acting in the opposite direction, $\Delta_{i\text{-}flexD,}$ as well as the rigid body deformation of the wall, $\Delta_{i\text{-}rigid}$, as given in Eqn. 3.1.

$$\Delta_i = \Delta_{i-flexI} - \Delta_{i-flexD} + \Delta_{i-rigid} \tag{3.1}$$

Since the wall is assumed to remain elastic at maximum response under the design level earthquake, each displacement shape included in Eqn. 3.1 can be obtained through the direct integration of its corresponding curvature distribution along the height of the wall. Therefore, $\Delta_{i\text{-}flexI}$, $\Delta_{i\text{-}flexD}$ and $\Delta_{i\text{-}rigid}$ are given by Eqns. 3.2, 3.3 and 3.4, respectively.

$$\Delta_{i-flexI} = \frac{F_e h_e}{6\,E_c I_g \sum_{j=1}^{N} h_j^2}\left[-\sum_{j=1}^{i-1} h_j^4 + 3\,h_i \sum_{j=1}^{i-1} h_j^3 + 3\,h_i^2 \sum_{j=i}^{N} h_j^2 - h_i^3 \sum_{j=i}^{N} h_j \right] \tag{3.2}$$

$$\Delta_{i-flexD} = \begin{cases} \dfrac{F_a h_b \cos\alpha}{3\,E_c I_g}\left(3\,h_i^2 - \dfrac{h_i^3}{h_b} \right) & for \quad h_i \le h_b \\ \dfrac{F_a h_b \cos\alpha}{3\,E_c I_g}\left(3\,h_b h_i - h_b^2 \right) & for \quad h_i > h_b \end{cases} \tag{3.3}$$

$$\Delta_{i-rigid} = \left(\theta_d - \frac{\Delta_{N-flexI} - \Delta_{N-flexD}}{h_N} \right) \cdot h_i \tag{3.4}$$

In the above equations, N is the total number of stories in the building, h_i, is the height of i^{th} seismic mass from the base of the wall, and θ_d is the design drift specified by the designer at the beginning of the design process and assumed constant along the height of the wall. When the displaced shape of the structure at maximum response is known, then the design displacement of the equivalent SDOF system, Δ_d, at the effective height, h_e, of the SDOF system can be obtained by Eqn. 3.5.

$$\Delta_d = \frac{\sum_{i=1}^{N} \left(m_i \Delta_i^2 \right)}{\sum_{i=1}^{N} \left(m_i \Delta_i \right)} \tag{3.5}$$

where m_i are the masses and Δ_i are the displacements at level i given by Eqn. 3.1. The effective mass of the SDOF system, M_e, participating in the fundamental mode of vibration at maximum response, as well as the effective height, h_e, are also established using the design displacement profile. As the second step in the design procedure, the design ductility factor of the equivalent SDOF system, μ, can be obtained by Eqn. 3.8. The yield displacement at the effective height of the structure, Δ_y, in this equation is based on an elastic linear displacement profile.

$$M_e = \frac{\sum_{i=1}^{N} \left(m_i \Delta_i \right)}{\Delta_d} \tag{3.6}$$

$$h_e = \frac{\sum_{i=1}^{N} \left(m_i \Delta_i h_i \right)}{\sum_{i=1}^{N} \left(m_i \Delta_i \right)} \tag{3.7}$$

$$\mu = \frac{\Delta_d}{\Delta_y} = \frac{\Delta_d h_w}{h_e \Delta_e} \tag{3.8}$$

The third step of the design procedure involves the determination of the equivalent viscous damping ratio at the design displacement. The overall equivalent viscous damping ratio of the system, ζ_{eq}, at the design displacement is the sum of the inherent elastic damping, ζ_e, and the hysteretic damping, ζ_h, dissipated during seismic response, as shown in Eqn. 4.9. In this equation, r is the post-uplift stiffness (slope of branch C-D in Fig. 2.1(b)), ζ_{ei} is the inherent damping ratio of the system based on its initial elastic properties, ζ_{ch} is the hysteretic damping computed from the hysteretic response of the PRW system at maximum response (see Fig. 2.1(b)) and f is a correction factor to better match nonlinear response (Priestley, 2007). Based on the closed-form solution obtained for the hysteretic response of PRWs, ζ_{ch} can be expressed as a function of the ductility ratio, μ, and the contribution ratio, λ, as given in Eqn. 3.9.

$$\zeta_{eq} = \zeta_e + \zeta_h = \sqrt{\frac{\mu}{1 + r\,\mu - r}}\,\zeta_{ei} + f\,\zeta_{ch} \tag{3.9}$$

As the fourth step of the design procedure, from the design displacement at maximum response, Δ_d, the effective period, T_e, can be obtained from the design displacement response spectrum at the corresponding equivalent damping ratio, ζ_{eq}, as illustrated in Fig. 3.1. The effective stiffness, K_e, of the equivalent SDOF system at maximum displacement (see Fig. 3.1) can then be obtained using the well-known SDOF expression of Eqn. 3.10. The design base shear force, V_b, is then simply obtained by Eqn. 3.11 and eventually, the design lateral force at each level i of the structure, F_i, is then obtained by Eqn.3.12.

$$K_e = 4\pi^2 M_e / T_e^2 \tag{3.10}$$

$$V_b = K_e \Delta_d \tag{3.11}$$

$$F_i = \frac{m_i \Delta_i}{\sum_{j=1}^{N} m_j \Delta_j} V_b \tag{3.12}$$

3.1. Iterative Numerical Design Procedure

The iterative DDBD procedure for PRWs starts with a number of predefined material properties and geometric characteristics for the PRW under design, as shown in Table 3.1. The iterative numerical design procedure for a given PRW aims at achieving the desired designed drift, θ_d, for a given design earthquake (DE) displacement response spectrum as well as satisfying simultaneously the following six performance objectives: 1) Full re-centering condition: $\lambda \geq 1$; 2) Elastic response of the prestressed reinforcement under the Maximum Considered Earthquake (MCE) defined as a multiplier (e.g. 1.5) of the amplitude of the DE: $f_{max\text{-}PT\text{-}MCE} \leq \alpha_o f_{y\text{-}PT}$, where $\alpha_o \leq 1.0$; 3) Elastic response of the concrete wall: wall sections are capacity designed to have a yield moment capacity greater than the amplified maximum bending moment demand at the DE level; 4) Damage control in hysteretic dampers: maximum damper displacement capacity is chosen as twice the MCE displacement demand; 5) Control of neutral axis depth as a ratio of the length of the wall: $c/l_w \leq 0.15$; and 6) Prevention of wall base sliding by proper design and/or detailing. The wall is considered to extend the full height of the building. An aspect ratio (h_w/l_w) between 3 and 6 is recommended for the concrete wall. The wall thickness, t_w, is selected to limit the average shear stress in the concrete under the design lateral forces between $3\sqrt{f_c'}$ and $5\sqrt{f_c'}$ per ACI 318-11 (ACI, 2011). The horizontal floor area needed to mount the diagonal steel props is governed by architectural constraints. Based on a parametric study conducted by the authors, in one of the first stages of the development of the DDBD procedure, it is recommended that an inclination angle between 60 and 70 degrees be selected for the steel props. Preferably, the steel props should be connected as close as possible to the top of the wall. The six main design parameters for PRWs to be determined from the iterative DDBD procedure include; 1) Initial

prestressing force in PT bars, R_i, 2) Activation/Yield force of hysteretic dampers, F_a, 3) Axial stiffness of steel props, k_b, 4) Cross-sectional area of PT bars, A_{PT}, 5) Neutral axis position, c, and 6) Maximum compressive strain in concrete, ε_c.

Table 3.1. Predefined structural parameters for DDBD of PRWs.

	Parameter	Description
Material Properties	f'_c	Compressive strength of unconfined concrete
	f_y	Yield strength of non-prestressed reinforcement
	f_u	Ultimate strength of non-prestressed reinforcement
	$f_{y\text{-}PT}$	Yield strength of prestressed reinforcement
	$f_{u\text{-}PT}$	Ultimate strength of non-prestressed reinforcement
Geometric Characteristics	h_W	Wall total height
	l_W	Wall length
	t_W	Wall thickness
	α	Steel props inclination angle
	h_b	Steel props vertical height
	h_e	Height of resultant first mode lateral force
	l_{PT}	Unbonded length of prestressed reinforcement

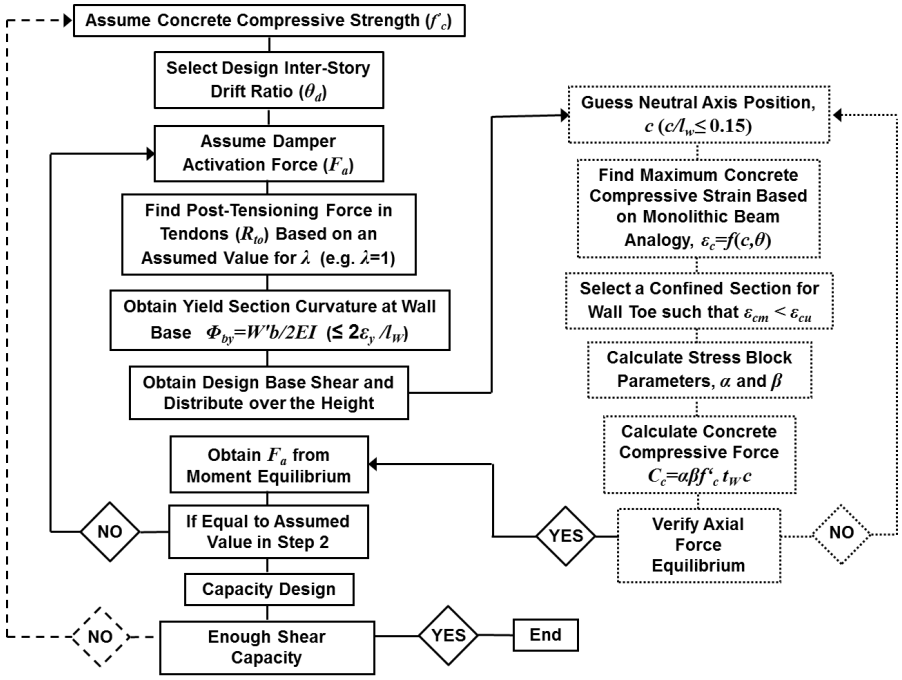

Figure 3.2. Flow chart for iterative numerical DDBD procedure for PRWs.

The DDBD methodology described here was embodied in an iterative numerical design procedure on the Matlab platform (Mathworks, 2011). Fig. 3.2 shows the flow chart of the design procedure. The DDBD procedure includes two main iterative loops. The loop on the right hand side of the flow chart seeks axial force equilibrium in the PRW. The inner loop on the left hand side of the flow chart seeks moment equilibrium. The final outer loop on the left hand side involves a standard capacity design procedure to avoid premature flexural and shear failures in the concrete wall at maximum response.

4. ON-GOING EXPERIMENTAL STUDY

As part of this research, the proposed design procedure and further the performance of PRWs are going to be evaluated through an on-going shake table testing program at the Structural Engineering and Earthquake Simulation Laboratory (SEESL) at University at Buffalo. For this purpose, a 1:3

scaled model has been designed and built and is about to undergo testing at the time of writing. The prototype building selected for this study is based on the re-designed form of the MCEER West Coast Demonstration Hospital (WC70) (Wang, 2007) assumed to be located in Southern California and meeting the requirements of a Seismic Design Category (SDC) D according to ASCE/SEI 7-10 (ASCE, 2010). The building is symmetric and has plan dimensions of 108' (32.9 m) by 24' (7.31 m), as illustrated in Fig 4.1. Two PRW units are introduced to provide lateral resistance in the north-south direction and are located symmetrically on each side of the building with respect to the center of gravity. Each propped concrete wall extends the full height of the building. Moreover, the passive supplemental damping devices used for the props in this case are selected to be in the form of Buckling-Restrained Braces (BRBs) (StarSeismic, LLC, 2012).

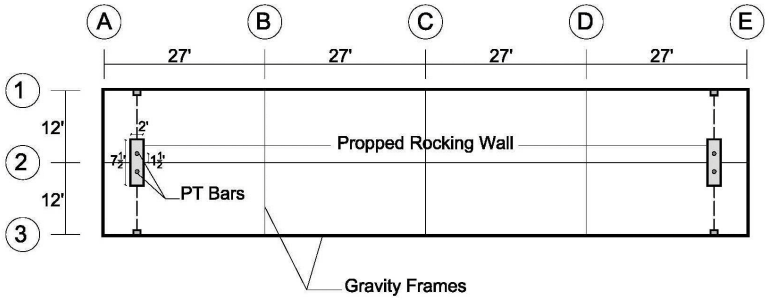

Figure 4.1. Plan view of the prototype structure (1 ft = 0.305 m)

The three-dimensional configuration of the test setup is shown in Fig. 4.2. The dimensional scale of the specimen is determined based on the limitations of the gravity frame system used to simulate the floor mass of the prototype structure. The Floor Mass Simulator (FMS) is composed of two adjacent frames supporting six steel plates, each weighing about 8.5 kips (37.8 kN). Due to the rocking support design at the base of its columns, the FMS performs as a pin-based structure in the direction of shaking, resulting in no lateral stiffness in this direction. The braces incorporated in the transverse direction, however, resist deformations in the direction perpendicular to the direction of shaking.

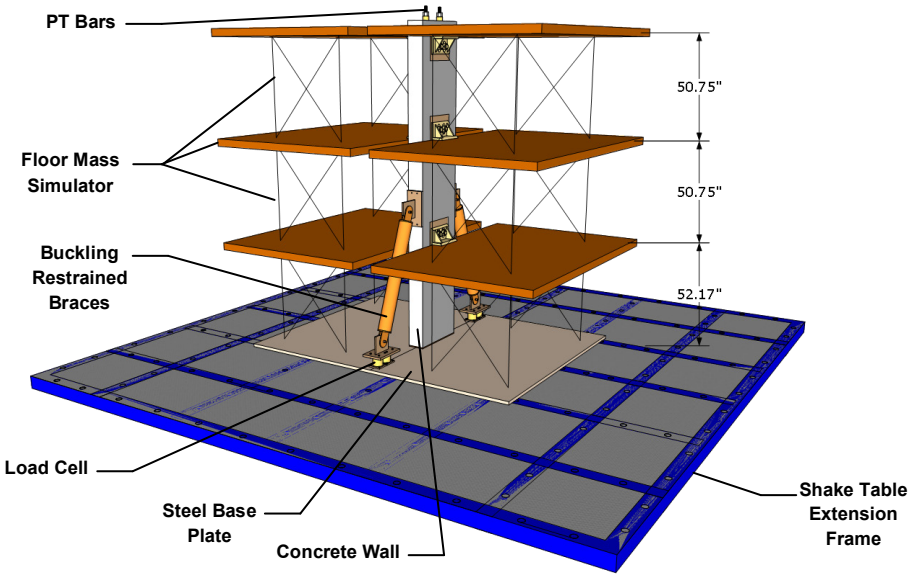

Figure 4.2. Schematic configuration of the test setup (the PRW specimen installed between two frames of the FMS) on the shake table (1 in. = 2.54 cm)

4.1. Design Results

Based on the similitude relationships, the concrete wall model is of 13' height with a thickness of t_w = 8 in. (20.3 cm) and a length of l_w = 30 in. (76.2 cm) The protraction of the props' axes intersect the

wall at the third floor (h_b = 7.27' = 2.21 m). The self-weight of the wall is W = 3.25 kips (14.5 kN) and the inclination of the BRBs to the horizontal is $\alpha = 69^o$. The non-prestressed reinforcement is of grade 60 (f_y = 60 ksi = 413.8 MPa) while the ultimate stress of the threaded bars used for the PT reinforcement is 150 ksi (1035 MPa). Assuming a 7.7 in. (19.6 cm) depth for the location of the PT anchorage underneath the surface of the extension frame on the shake table, the overall unbonded length of the PT reinforcement becomes l_{PT} = 13.65' (4.16 m). In order to minimize damage in the wall and provide vertical equilibrium against the axial forces due to the PT bars and the self-weight of the wall at the design drift, high strength concrete with a 28-day compressive strength f'_c = 6 ksi (41.4 MPa) is considered. Based on the tributary area between the PRWs, the seismic weight for each PRW is 17.12 kips (76.2 kN) at each floor level of the test building.

The building is assumed to be located on a site with short and 1-sec period design spectral values of S_{DS} = 1.0g and S_{D1} = 0.6g, respectively, according to ASCE/SEI 7-10 (ASCE, 2010). In order to design the building for a seismic performance significantly above code-design level, a target design story drift of 1% (θ_d = 0.01) under the design level (DE) ground motion was selected. This design drift along with the six performance objectives stated above must be satisfied simultaneously by the DDBD procedure. A contribution ratio λ = 1 (see Eqn. 2.1) is selected in order to control the self-centering response of the system while at the same time maximizing the energy dissipation by the BRBs at the design story drift. Table 4.1 provides the resulting design properties of the PRWs following the iterative DDBD procedure using the Matlab platform. The effective fundamental period of the PRW was computed as T_e = 0.44 sec, and the equivalent damping ratio at the design drift was computed as ζ_{eq} = 12.7% of critical which was composed of 10.3% of hysteretic damping and 2.4% of inherent elastic damping (see Eqn. 3.9).

Table 4.1. Resulting design properties for the three-story PRW test model.

No.	Parameter	Description	Unit	Design Value
1	R_i	Initial prestressing force in PT reinforcement (per bar)	kN	311.8
2	F_a	Activation force of BRBs	kN	38.0
3	k_b	Axial stiffness of steel props	kN/m	23.1E+3
4	A_{PT}	Cross-sectional area of PT reinforcement (per bar)	cm^2	8.1
5	c	Neutral axis position	cm	7.9
6	ε_c	Maximum compressive strain in concrete	-	0.0033
7	ρ_l	Longitudinal reinforcement ratio	%	1.8

4.2. Numerical Model

A numerical model of the PRW structure designed for the shake table testing is developed in PERFORM 3D v4 (Computers and Structures, 2003). The concrete wall panel is modeled using fiber elements. The smooth stress-strain relationships of the unconfined concrete and the confined concrete are based on the model developed by Mander *et al*. (1988). A set of eleven nonlinear elastic gap elements is introduced at the base of the wall in order to model the gap opening at this section. These contact elements provide zero stiffness in tension and very high stiffness in compression. The braces are modeled using the BRB inelastic bar type components which account for the isotropic hardening of the buckling restrained braces based on the maximum axial deformation in such elements. The PT steel bars are modeled using an inelastic steel tie element with inelastic tension-only steel material. The stress-strain relationship of the material used for this element is a tri-linear idealization of the smooth stress-strain relationship of the PT steel with a strength loss at the point of rupture.

4.3. Earthquake Ground Motions

The earthquake ground motions selected for the numerical study were 10 of the 44 historical motions of the FEMA P695 far field ground motion set (FEMA, 2009). The ten ground motions were selected to have similar values as the complete P695 motion set for several selected statistical spectral parameters of interest (median, arithmetic mean, geometric mean and standard deviation) within the period range of interest (Sideris *et al*., 2010). Table 4.2 summarizes the characteristics of the

similitude-scaled reduced earthquake ensemble used in the nonlinear response analyses. According to the P695 Methodology, the ground motions were scaled such that their 5% damped median spectral acceleration at the elastic fundamental period of the PRW (0.18 sec) matches that of the ASCE/SEI 7-10 response spectrum for the design spectral values of S_{DS} = 1.0g and S_{D1} = 0.6g, respectively. The resulting scaling factor for all ten ground motions was 0.47.

Table 4.2. Characteristics of reduced P695 ground motion ensemble to be used in experimental study (unscaled).

EQ Index	EQ ID	Earthquake	Year	Mag.	Station	Fault Type	PGA (g)
4	120122	Northridge	1994	6.7	Canyon Country-W Lost Cany	Blind thrust	1.35
9	120611	Imperial Valley	1979	6.5	Delta	Strike-slip	1.55
19	120821	Kocaeli, Turkey	1999	7.5	Arcelik	Strike-slip	1.01
20	120822	Kocaeli, Turkey	1999	7.5	Arcelik	Strike-slip	1.01
21	120911	Landers	1992	7.3	Yermo Fire Station	Strike-slip	0.80
24	120922	Landers	1992	7.3	Coolwater	Strike-slip	1.52
25	121011	Loma Prieta	1989	6.9	Capitola	Strike-slip	1.47
30	121112	Manjil, Iran	1990	7.4	Abbar	Strike-slip	1.35
36	121322	Cape Mendocino	1992	7.0	Rio Dell Overpass – FF	Thrust	2.82
39	121421	Chi-Chi, Taiwan	1999	7.6	TCU045	Thrust	0.97

4.4. Response History Analyses Results

Two dimensional Nonlinear Response History Analyses (NRHA) of the PRW test model were conducted on the PERFORM 3D v4 platform under each of the ten ground motions described above at the DE and MCE intensity levels (defined in this study as 1.5 times the amplitude of the DE level). Inherent viscous damping ratios of 2% and 5% of critical were assigned to the fundamental and higher modes of vibration, respectively. Figures 4.3 and 4.4 illustrate the numerical predictions of the performance of the test model at both DE and MCE levels of intensity.

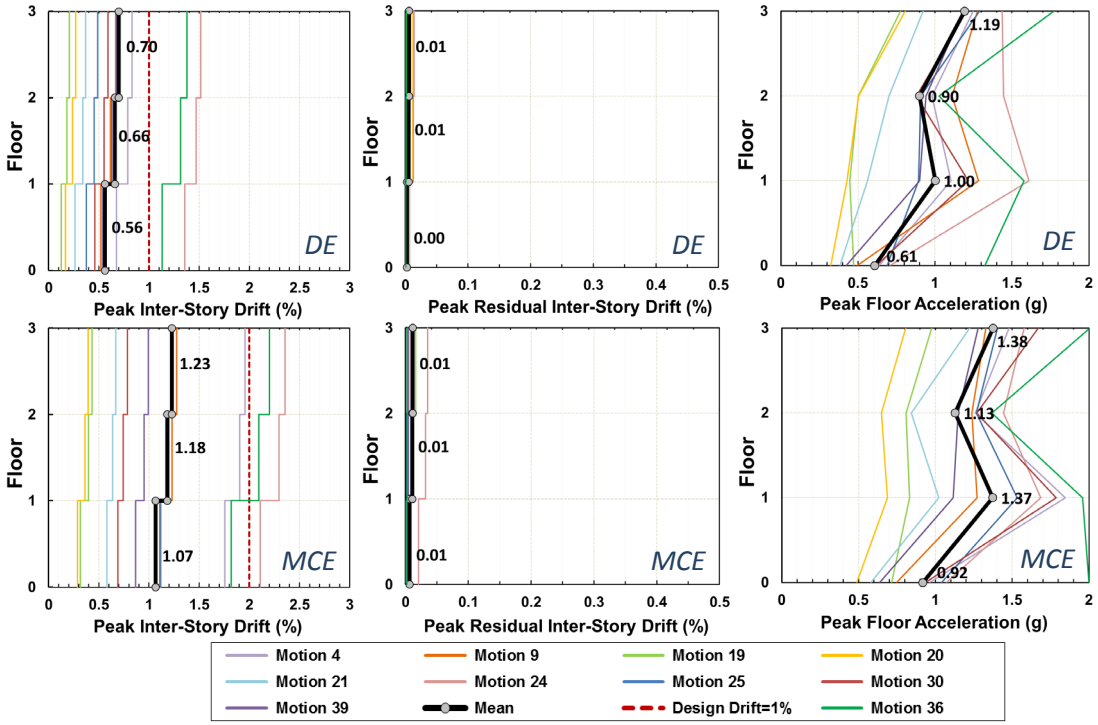

Figure 4.3. Peak story drifts, peak residual story drifts and peak absolute floor accelerations for PRW under design (DE) and maximum considered (MCE) earthquake ground motions.

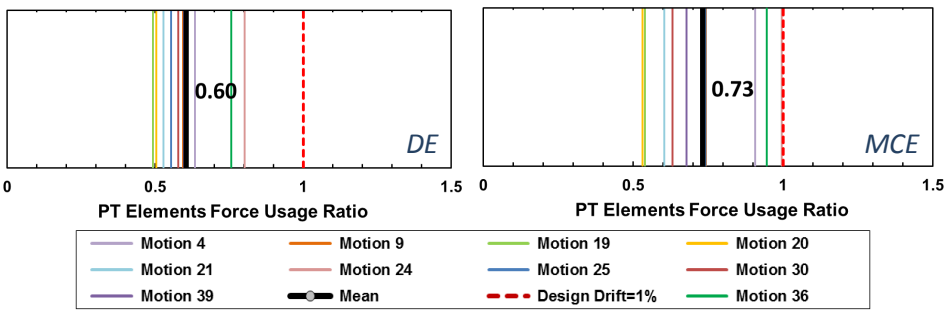

Figure 4.4. PT Elements force usage ratios for PRW under design (DE) and maximum considered (MCE) earthquake ground motions.

The effectiveness of the proposed DDBD procedure to achieve the design performance objectives is confirmed by the result shown in Figs. 4.3 and 4.4. The average peak inter-story drift envelopes at both DE and MCE levels (indicated as a solid black lines) are less than the target drifts (indicated as a dotted red lines). The PRW system remains damage free at the DE level, while the shear and moment capacities for the wall provide enough safeguards against collapse at the MCE level.

5. CONCLUSIONS

In this paper, a Direct Displacement-Based Design (DDBD) procedure is proposed for a novel seismic force resisting-system incorporating Propped Rocking Walls (PRWs). The effectiveness of the proposed design procedure as well as the performance of PRWs was conformed numerically. An on-going shake table testing program is now aimed at verifying experimentally the seismic performance of PRWs.

AKCNOWLEDGEMENT

The authors would like also to thank David Mar, S.E., from Tipping Mar & Associates, Berkeley, CA, U.S.A., for his collaboration in the initial phases of this research work and StarSeismic, LLC for donating the buckling-restrained braces to be used in the exprimental study.

REFERENCES

American Concrete Institute (2011), ACI 318-11: Building Code Requirements for Structural Concrete and Commentary. Farmington Hills, MI, U.S.A.

American Society of Civil Engineers (2010). ASCE Standard ASCE/SEI 7-10: Minimum Design Loads for Buildings and other Structures. Reston, VA, U.S.A.

Fathali, S. (2009). Personal Communications.

Mander, J. B., Priestley, M. J. N. and Park, R. (1988). Observed Stress-Strain Behavior of Confined Concrete. *Journal of Structural Engineering*. **114**, 1827-1849.

Priestley, M. J. N. (1993). Myths and Fallacies in Earthquake Engineering – Conflicts between Design and Reality. *Bulletin of NZ National Society for Earthquake Engineering*. New Zealand, **26**, 329-341.

Priestley, M. J. N., Calvi, G. M. and Kowalsky, M. J. (2007). Displacement Based Seismic Design of Structures. IUSS Press, Pavia, Italy.

Sideris, P., Filiatrault, A., Leclerc, M. and Tremblay, R. (2010). Experimental Investigation on the Seismic Behavior of Palletized Merchandise in Steel Storage Racks. *Earthquake Spectra.* **26**, 209-233.

StarSeismic, LLC. (2012). Park City, UT, U.S.A. Web: www.starseismic.net

Wang, D. (2007). Numerical and Experimental Studies of Self-Centering Post-Tensioned Steel Frames. *Ph.D. Dissertation*. State University of New York at Buffalo, Buffalo, NY, U.S.A.

Wolfe, J., Mar, D. and Tipping, S. (2001). Propped Shear Walls; Combining Steel Braces And Concrete Shear Walls for Seismic Strengthening of Existing Buildings. *Modern Steel Construction*. **January 2001**, 5 p.